

Accepted Manuscript

Synthesis and biological characterization of organoruthenium complexes with 8-hydroxyquinolines

Jakob Kljun, Ignacio E. León, Špela Peršič, Juan F. Cadavid-Vargas, Susana B. Etcheverry, Weijiang He, Yang Bai, Iztok Turel



PII: S0162-0134(18)30044-8
DOI: doi:[10.1016/j.jinorgbio.2018.05.009](https://doi.org/10.1016/j.jinorgbio.2018.05.009)
Reference: JIB 10499

To appear in: *Journal of Inorganic Biochemistry*

Received date: 22 January 2018
Revised date: 24 April 2018
Accepted date: 16 May 2018

Please cite this article as: Jakob Kljun, Ignacio E. León, Špela Peršič, Juan F. Cadavid-Vargas, Susana B. Etcheverry, Weijiang He, Yang Bai, Iztok Turel, Synthesis and biological characterization of organoruthenium complexes with 8-hydroxyquinolines. The address for the corresponding author was captured as affiliation for all authors. Please check if appropriate. Jib(2017), doi:[10.1016/j.jinorgbio.2018.05.009](https://doi.org/10.1016/j.jinorgbio.2018.05.009)

This is a PDF file of an unedited manuscript that has been accepted for publication. As a service to our customers we are providing this early version of the manuscript. The manuscript will undergo copyediting, typesetting, and review of the resulting proof before it is published in its final form. Please note that during the production process errors may be discovered which could affect the content, and all legal disclaimers that apply to the journal pertain.

Synthesis and biological characterization of organoruthenium complexes with 8-hydroxyquinolines

Jakob Kljun¹, Ignacio E. León^{2,3}, Špela Peršič¹, Juan F. Cadavid-Vargas^{2,3}, Susana B. Etcheverry^{2,3}, Weijiang He⁴, Yang Bai⁴, Iztok Turel^{1,*}

¹ Faculty of Chemistry and Chemical Technology, University of Ljubljana, Večna pot 113, 1000 Ljubljana, Slovenia, iztok.turel@fkkt.uni-lj.si

² Chair of Pathologic Biochemistry, Exact School Sciences, National University of La Plata, 47 y 115, 1900 La Plata, Argentina. E-mail: etcheverry@biol.unlp.edu.ar

³ Inorganic Chemistry Center (CEQUINOR, CONICET), Exact School Sciences, National University of La Plata, 47 y 115, 1900 La Plata, Argentina

⁴ State Key Laboratory of Coordination Chemistry, School of Chemistry and Chemical Engineering, Nanjing, 210017, People's Republic of China

Abstract

In this study we report the synthesis, characterization and a thorough biological evaluation of twelve organoruthenium–8-hydroxyquinolinato (**Ru-hq**) complexes. The chosen **hqH** ligands bear various halogen atoms in different positions which enables to study effect of the substituents on physico-chemical and biological properties. The determined crystal structures of novel complexes expectedly show the cymene ring, a bidentately coordinated deprotonated **hq** and a halide ligand (chlorido or iodido) coordinated to the ruthenium central ion. In previous studies the anticancer potential of organoruthenium complex with 8-hydroxyquinoline ligand clioquinol was well established and we have decided to perform an extended biological evaluation (antibacterial and antitumor activity) of the whole series of halo-substituted analogs. Beside the cytotoxic potential of studied compounds also the effect of two selected complexes (**9** and **10**) on apoptosis induction in MG-63 and A549 cells was also studied via externalization of phosphatidylserine at the outer plasma membrane leaflet. Both selected complexes that gave best preliminary cytotoxicity results contain bromo substituted **hq** ligands. Apoptosis induction results are in agreement with the cell viability assays suggesting the higher and more selective anticancer activity of complex **10** in comparison to complex **9** on MG-63 cells.

1. Introduction

The development of novel cancer metallodrugs is driven by the complexities of presently used chemotherapeutic approaches and several issues that such treatment presents, for example intrinsic and acquired resistance and common as well as severe side-effects. Metal based scaffolds offer us novel opportunities of drug design in terms of building block arrangements and geometries and the possibility of direct metal-target interactions beside conventional covalent and supramolecular interactions.[1]

One of the strategies employed in metal-based drug design is the binding of metal fragments to known pharmacophores such as 8-hydroxyquinolines.[2] This class of compounds is well known for their wide range of clinical applications ranging from antibacterial, antifungal and antiviral agents to disinfectants and antiseptics.[3, 4] These compounds and their derivatives are present in a large number of preclinical studies and exert promising antiparasitic, antimalarial and anticancer effects.[4-7] Their action is often attributed to the interaction with metal species including copper, zinc and iron cations which are relatively abundant in biological systems and is often dependent on their concentration.[4-7]

The most successful example of this strategy is the case of antimalarial ferrocene-quinoline conjugates where its main representative – ferroquine – is the most advanced organometallic drug candidate having successfully completed phase II clinical trials.[8-11] Conjugation of bioactive molecules to organoruthenium species has previously proven a successful strategy for obtaining novel metallodrugs.[1, 12-17] Our group has employed this strategy previously in the case of antiviral nucleoside analogues,[18, 19] antibacterial quinolones,[20-22] azole antifungal agents,[23] pyriithione[24] and most importantly 8-hydroxyquinoline agent clioquinol (**Figure 1**).[25, 26]

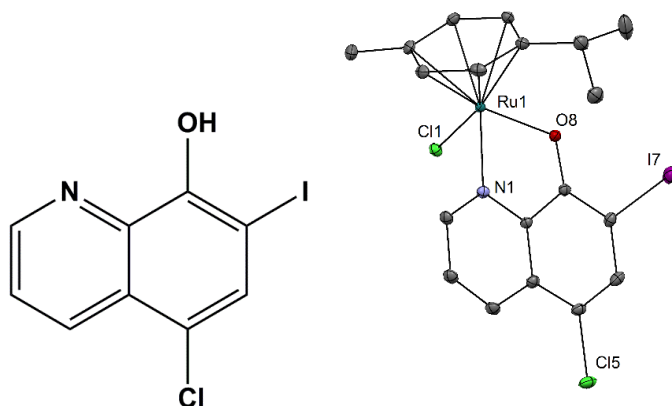


Figure 1: Clioquinol (cqH) and its organoruthenium complex $[\eta^6\text{-p-cymene})\text{Ru}(\text{cq})\text{Cl}]$ [26].

Clioquinol (cqH) is one of many 8-hydroxyquinolines used in clinical practice. These compounds were first used as broad spectrum antimicrobial agents, however, their use is nowadays somewhat limited as disinfecting or antiseptic agents. Clioquinol itself has completed phase II clinical trials as prospective agent against Alzheimer's disease[27] but the studies were not continued due to difficulties in large scale synthesis. Both clioquinol and other hydroxyquinolines have been used as ligands in the design of metallodrugs due to the stability and favorable physico-chemical properties of their coordination compounds.[28-30]

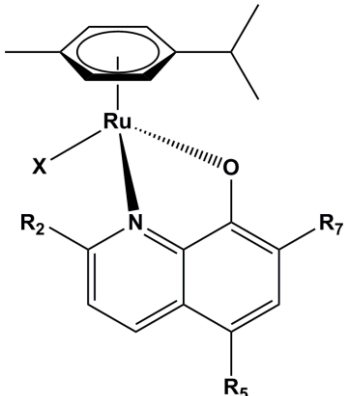
In 2014 our group has reported the synthesis and biological evaluation of the organoruthenium-clioquinol complex with the formula $[(\eta^6\text{-p-cymene})\text{Ru}(\text{clioquinolato})\text{Cl}]$ (**Figure 1**).[26] It was established that the complex induces caspase-dependent cell death which is observed at much lower concentrations in leukaemic cell lines than in cell lines of solid tumors. Moreover, the complex showed proteasome-independent inhibition of the NF κ B signaling pathway with no effects on cell-cycle distribution which suggest a mode of action altogether different from the free clioquinol ligand itself. Encouraged by the promising results and the favorable toxicologic profile of this complex we have performed an in-depth investigation of the mode-of-action including the interactions with possible molecular targets.[25] We have discovered that the organoruthenium-clioquinol complex is a potent inhibitor of the lysosomal cysteine protease cathepsin B, an enzyme involved in tumor cell invasion and metastasis. While the complex did not show cytotoxic effects in low micromolar concentration range on MCF-10A neoT (breast cancer) and U-87 MG (glioma) cell lines which both express high levels of proteolytically active cathepsin B it

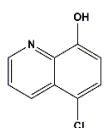
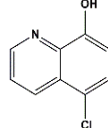
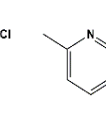
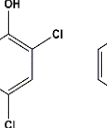
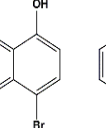
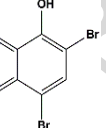
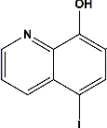
significantly reduced their ability for extracellular matrix degradation and invasiveness in two independent cell-based models.[31]

Some of the organoruthenium complexes of clioquinol and 5,7-dihalosubstituted 8-hydroxyquinolines presented here were also studied by the Hartinger group (compounds **2**, **5**, **7**, **10**, **11** in this study).[32] It was found that the leaving halogenido ligand plays a contributing role in the toxicity profile and surprisingly the cellular accumulation rates do not play a major role in it.[32] The compounds are stable in dmsO and aqueous solutions at a wide range of pH levels. They readily react with histidine, 9-ethylguanine and guanosine 5'-monophosphate to form adducts. Interestingly, the complexes do not interact with methionine while the presence of cysteine causes the cleavage of the cymene ring. Altogether, the compounds displayed very similar toxicities towards the tested cancer cell lines (HCT116 colon cancer, NCI-H460 carcinoma, SiHa cervical cancer) with IC₅₀ values in the low micromolar range.

Another study of Malipeddi *et al.*[33] was recently published involving organoruthenium complexes and their antibacterial properties. However, this study in absence of structural data proposes incorrect structures of the synthesized complexes (**1**, **2**, **5**) in which the hqH ligand is presumed to be coordinated in a neutral form. The study offers no evidence to support this assumption and is contrary to both the expected chemistry of hydroxyquinolines as well as the previous findings of Thai *et al.*,[34] Hartinger *et al.*[32] and ourselves which prove the coordination of the ligands in monoanionic form also when the synthesis is carried out in absence of base (though resulting in lower yields).

Herein, we offer a wholesome study of the ruthenium-hydroxyquinolinato system which includes the synthetic procedure for reliable and high-yield synthesis of organoruthenium 8-hydroxyquinolinato complexes, their physico-chemical characterization as well as an extended biological evaluation of a series of organoruthenium-8-hydroxyquinolinato complexes (four new and eight previously published).

Table 1: Ruthenium complexes included in this study.


							
X =	1 [33,	2 [32-34]	3 [34]	4	5 [32, 33]	/	Ru-Cq [26]
Cl	34]						
X =	6	7 [32]	8	9	10 [32]	11 [32]	12 [32]
I							

2. Materials and methods

2.1 Materials

The ruthenium-cymene precursors (chlorido – **P1**, iodido – **P2**), hydroxyquinoline ligands and solvents were purchased from Strem chemicals, Sigma-Aldrich and/or Fluorochem and were used as received. The solvents used in the spectroscopic study were of spectral grade from Tedia Company Inc.. Tris(2,2'-bipyridine)ruthenium dichloride ($[\text{Ru}(\text{bpy})_3]\text{Cl}_2$) and 1,3-Diphenylisobenzofuran (DPBF) used in singlet oxygen generate (SOG) quantum yield detection was purchased from Energy Chemical, China.

Tissue culture materials were purchased from Corning (Princeton, NJ, USA), Dulbecco's modified Eagle's medium (DMEM) and TrypLE™ were purchased from Gibco (Gaithersburg, MD, USA), and fetal bovine serum (FBS) was purchased from Internegocios (Argentina). Annexin V, fluorescein isothiocyanate (FITC), and propidium iodide (PI) were from Invitrogen (Buenos Aires, Argentina). All other chemical were from Sigma (St. Louis, MO, USA). The MG-63 and A549 cell lines were purchased from ATCC (American Type Culture Collection),

2.2 Methods

Syntheses

General procedure for the synthesis of complexes **1-12**.

40-80 mg of appropriate ruthenium precursor (**P1/P2**) was suspended in 30 mL of acetone. After 10 min of stirring and gentle heating 2.06 molar equivalents of hydroxyquinoline ligand and 1.96 molar equivalents of base (NaOMe or NaOAc·3H₂O) were added to the reaction mixture and the mixture was stirred overnight at room temperature. The turbid solution was filtered over celite to remove the precipitated inorganic salts and concentrated to 3-5 mL. The addition of 20 mL of cold *n*-heptane resulted in yellow-brown precipitates. Formation of oily products was avoided by drying solvents with sodium sulfate and 4Å molecular sieves if necessary. A common impurity present in precipitates are starting ruthenium precursors (indicated by the pale reddish color of the heptane mother solution after product precipitation) and unreacted/excess hydroxyquinoline ligands. The products can easily be purified by flash chromatography on silica where 3 % and 20 % acetone/DCM mixtures are used as eluents for excess ligand and Ru-hq complex respectively (R_f for precursor/ligand/complex are 0/0.60-0.70/0.05 and 0.05/0.90/0.50-0.70 respectively). Crystals suitable for X-ray diffraction were obtained by slow evaporation of a CHCl₃/heptane solution for **1**, **6**, **7**, and **9** and a CHCl₃/MeOH solution for **11**.

Characterization

Attenuated total reflectance (ATR) infrared spectra were recorded on a Perkin-Elmer Spectrum 100 spectrometer. The measurements were made in the range from 4000 cm⁻¹ to 600 cm⁻¹. Elemental analyses were performed on a Perkin-Elmer 2400 CHN Elemental analyzer. X-ray diffraction data were collected on an Oxford Diffraction SuperNova diffractometer with a Cu microfocus X-ray source, with mirror optics and an Atlas detector. The structures were solved using SIR92.[35] Full-matrix least-squares refinement on the F magnitudes with anisotropic displacement factors for all of the non-hydrogen atoms used SHELXL.[36] The drawings and the analysis of bond lengths, angles and intermolecular interactions were carried out using Mercury and Platon.[37] Hydrogen atoms were placed

in geometrically calculated positions and were refined using a riding model. NMR spectra were recorded on a Bruker Avance III 500 spectrometer. Fluorescence spectra were determined using a Horiba FluoroMax-4 spectrofluorometer and fluorescence quantum yields were determined using an integrating sphere with absorbance of samples at their respective excitation wavelengths being lower than 0.05. Absorbance of samples in fluorescence quantum yields and singlet oxygen generate quantum yield detection were determined on a Perkin Elmer E35 spectrophotometer. The crystal structures were deposited in the CCDC database and were assigned the following deposition numbers; 1584336-40.

2.3 Experimental data

Spectral data of previously reported compounds (**1**, **2**, **3**, **5**, **7**, **10**, **11**, **12**) are in accordance with published data. Measurements are included in the SI.

[η^6 -*p*-cymene)Ru(5-bromo-8-hydroxyquinolato)Cl] (4)

39.4 mg **P1** (0.064 mmol), 30.0 mg 5-bromo-8-hydroxyquinoline (0.133 mmol), 17.1 mg NaOAc·3H₂O (0.126 mmol). Yield: 55.5 (87.3 %).

¹H NMR (500 MHz, Chloroform-*d*): δ 8.93 (s, 1H), 8.36 (d, *J* = 8.0 Hz, 1H), 7.53 (d, *J* = 8.0 Hz, 1H), 7.44 (d, *J* = 5.4 Hz, 1H), 6.91 (d, *J* = 5.4 Hz, 1H), 5.62 (s, 1H), 5.49 (s, 1H), 5.44 (s, 1H), 5.32 (s, 1H), 2.78 (sept, *J* = 7.7 Hz, 1H), 2.31 (s, 3H), 1.16 (2d, *J* = 7.7 Hz, 6H).

UV-Vis (λ [nm], ϵ [Lmol⁻¹cm⁻¹], *c* = 7.0·10⁻⁵ mol/L, CH₂Cl₂): 355 nm (0.2660), 437 nm (0.2844).

Selected IR peaks (cm⁻¹): 1739, 1568, 1495, 1457, 1378, 1357, 1319, 1217, 1203, 818, 654.

CHN for C₁₉H₁₉BrClNORu: calcd. C 46.22, H 3.88, N 2.84; exp. C 45.99, H 3.58, N 2.97.

[η^6 -*p*-cymene)Ru(5-chloro-8-hydroxyquinolato)I] (6)

78.5 mg **P2** (0.080 mmol), 30.0 mg 5-chloro-8-hydroxyquinoline (0.165 mmol), 21.4 mg NaOMe (0.157 mmol). Yield: 85.0 mg (97.9 %). Compound is slightly hygroscopic.

¹H NMR (500 MHz, Chloroform-*d*): δ 8.90 (dd, $J = 4.9, 1.2$ Hz, 1H), 8.39 (dd, $J = 8.6, 1.2$ Hz, 1H), 7.44 (dd, $J = 8.6, 4.9$ Hz, 1H), 7.39 (d, $J = 8.6$ Hz, 1H), 6.93 (d, $J = 8.6$ Hz, 1H), 5.58 – 5.53 (m, 2H), 5.53 – 5.47 (m, 1H), 5.37 (d, $J = 5.8$ Hz, 1H), 2.96 (p, $J = 6.9$ Hz, 1H), 2.44 (s, 3H), 1.25 (d, $J = 6.9$ Hz, 3H), 1.23 (d, $J = 7.0$ Hz, 3H).

UV-Vis (λ [nm], ϵ [Lmol⁻¹cm⁻¹], $c = 3.5 \cdot 10^{-5}$ mol/L, CH₂Cl₂): 342 nm (0.1751), 446 nm (0.1614).

Selected IR peaks (cm⁻¹): 1738, 1562, 1455, 1373, 1360, 1320, 815, 773, 747, 676, 624.

CHN for C₁₉H₁₉ClINORu: calcd. C 42.20, H 3.54, N 2.59; exp. C 42.58, H 3.66, N 2.61.

[η^6 -*p*-cymene)Ru(2-methyl-5,7-dichloro-8-hydroxyquinolinato)I] (**8**)

40.8 mg **P2** (0.042 mmol), 25.5 mg 2-methyl-5,7-dichloro-8-hydroxyquinoline (0.110 mmol), 14.3 mg NaOAc·3H₂O (0.105 mmol). Yield: 40 mg (98.3 %).

¹H NMR (500 MHz, Chloroform-*d*): δ 8.20 (d, $J = 8.6$ Hz, 1H), 7.41 (s, 1H), 7.35 (d, $J = 8.6$ Hz, 1H), 5.68 (s, 1H), 5.64 (s, 1H), 5.48 (d, $J = 5.7$ Hz, 1H), 5.21 (d, $J = 5.7$ Hz, 1H), 3.13 (s, 3H), 2.87 – 2.76 (m, 1H), 2.60 (s, 3H), 1.19 (d, $J = 7.0$ Hz, 3H), 0.98 (d, $J = 6.9$ Hz, 3H).

UV-Vis (λ [nm], ϵ [Lmol⁻¹cm⁻¹], $c = 6.8 \cdot 10^{-5}$ mol/L, CH₂Cl₂): 345 nm (0.2755), 437 nm (0.2167).

Selected IR peaks (cm⁻¹): 1621 1546, 1451, 1426 1360, 881, 828, 778, 758, 704, 665.

CHN for C₂₀H₂₀Cl₂INORu: calcd. C 40.77, H 3.42, N 2.38; exp. C 40.29, H 3.11, N 1.98.

[η^6 -*p*-cymene)Ru(5-bromo-8-hydroxyquinolinato)I] (**9**)

62.9 mg **P2** (0.064 mmol), 30.0 mg 5-bromo-8-hydroxyquinoline (0.133 mmol), 17.1 mg NaOAc·3H₂O (0.126 mmol). Yield: 70 mg (93 %).

¹H NMR (500 MHz, Chloroform-*d*): δ 8.86 (dd, $J = 5.0, 1.2$ Hz, 1H), 8.32 (dd, $J = 8.6, 1.2$ Hz, 1H), 7.52 (d, $J = 8.6$ Hz, 1H), 7.40 (dd, $J = 8.6, 5.0$ Hz, 1H), 6.87 (d, $J = 8.6$ Hz, 1H), 5.52 (2d, $J = 6.0$ Hz, 2H), 5.48 (d, $J = 6.0$ Hz, 1H), 5.34 (d, $J = 6.0$ Hz, 1H), 2.94 (sept, $J = 6.9$ Hz, 1H), 2.41 (s, 3H), 1.22 (d, $J = 6.9$ Hz, 3H), 1.20 (d, $J = 6.9$ Hz, 3H).

UV-Vis (λ [nm], ϵ [Lmol⁻¹cm⁻¹], $c = 4.5 \cdot 10^{-5}$ mol/L, CH₂Cl₂): 341 nm (0.2036), 446 nm (0.1923).

Selected IR peaks (cm⁻¹): 1739, 1562, 1493, 1450, 1357, 1317, 1218, 1205, 820, 645.

CHN for C₁₉H₁₉BrINORu: calcd. C 38.99, H 3.27, N 2.39; exp. C 38.73, H 2.97, N 2.62.

Fluorescence measurements

Table 2: Fluorescent properties of **5** and **11**.

Cpd.	Solvent	λ_{ex}	λ_{em}	Φ^a /%
5	CH ₂ Cl ₂	355	424	0.06
	MeCN	270	409	N.d. ^b
	MeOH	290	416	N.d. ^b
	DMSO	360	402	N.d. ^b
11	CH ₂ Cl ₂	350	425	N.d. ^b
	MeCN	270	415	N.d. ^b
	MeOH	270	416	N.d. ^b
	DMSO	360	424	N.d. ^b

^a Fluorescent quantum yields are calculated using integrating sphere. ^b Lower than 0.01 %.

Singlet oxygen generate (SOG) quantum yield measurement

DPBF (1,3-Diphenylisobenzofuran, 10 μM) was dissolved in MeCN and its absorption spectra were recorded. Ruthenium complexes (10 μM) were then added to the solution and absorption spectra were recorded after laser irradiation (450 nm) individually. The absorbance at 411 nm (λ_{411}) indicates the DPBF absorption and the differentiation with that of unirradiated sample were recorded versus irradiation time. Then the slopes can be obtained which stand for the SOG efficiency. The SOG efficiencies can be calculated compared to the reference sample tris(2,2'-bipyridine) ruthenium dichloride.

Cell line and growth conditions

MG-63 human osteosarcoma cells, A549 human lung adenocarcinoma cells and MRC-5 human fibroblast were grown in DMEM containing 10 % FBS, 100 U/mL penicillin, and 100 $\mu\text{g}/\text{mL}$ streptomycin at 37° C in a 5 % CO₂ atmosphere. Cells were seeded in a 75-cm² flask, and when 70–80 % of confluence was reached, cells were subcultured using 1 mL of TrypLE™ per 25-cm² flask. For experiments, cells were grown in multiwell plates. When cells reached the desired confluence, the monolayers were washed with DMEM and were incubated under different conditions according to the experiments.

Cell viability study: 3-(4,5-Dimethylthiazol-2-yl)-2,5-diphenyltetrazolium bromide assay

The 3-(4,5-dimethylthiazol-2-yl)-2,5-diphenyltetrazolium bromide (MTT) assay was performed according to Mosmann.[38] Briefly, cells were seeded in a 96-well dish, allowed to attach for 24 h, and treated with different concentrations of Ru compounds at 37° C for 1, 3, 6 and 24 h. Afterward, the medium was changed and the cells were incubated with 0.5 mg/mL MTT under normal culture conditions for 3 h. Cell viability was marked by the conversion of the tetrazolium salt MTT to a colored formazan by mitochondrial dehydrogenases. Color development was measured spectrophotometrically with a microplate reader (model 7530, Cambridge Technology, USA) at 570 nm after cell lysis in DMSO (100 µL per well). Cell viability was plotted as the percentage of the control value.

Measurement of externalization of phosphatidylserine by annexin V-FITC/PI staining

Cells in early and late stages of apoptosis were detected with annexin V-FITC and PI staining. Cells were treated with 10, 25 and 100 µM of Ru complexes and were incubated for 3 and 6 h prior to analysis. For the staining, cells were washed with PBS and adjusted to a concentration of $1 \cdot 10^6$ cells per milliliter in 1X binding buffer. To 100 µL of cell suspension, 2.5 µL of annexin V-FITC was added and the mixture was incubated for 15 min at room temperature. Finally, 2 µL PI (250 µg/mL) was added prior to analysis. Cells were analyzed using flow cytometer (BD FACS Calibur™) and FlowJo 7.6 software. For each analysis, 10,000 counts, gated on a forward scatter versus side scatter dot plot, were recorded. Four subpopulations were defined in the dot plot: the undamaged vital (annexin V negative/PI negative), the vital mechanically damaged (annexin V negative/PI positive), the apoptotic (annexin V positive/PI negative), and the secondary necrotic (annexin V positive/PI positive) subpopulations.

Antibacterial activity

The in vitro antibacterial activity of the synthesized compounds was carried out using Escherichia coli (Gram negative), Bacillus cereus (Gram positive) and Staphylococcus Aureus (Gram positive) bacterial strains. The MICs of some synthesized compounds against three bacterial strains were evaluated using the micro-broth dilution method using

Muller-Hinton broth in tubes. The test compounds were first dissolved in DMSO and then diluted with sterile water (0.78-13.6 $\mu\text{g/ml}$). Bacterial suspension (10^6 cfu/mL) was then added to each tube and the tube set aside for incubation. After incubation for 24 h at 37 °C, MICs were measured. Three replicates were performed for each experiment.

3. Results and discussion

3.1 Syntheses and characterization

Previous studies present several different synthetic methods for preparation of ruthenium hydroxyquinoline complexes including the two-step synthesis via preparation of the sodium hydroxyquinolinato salts or several solvent changes. Here we present a one-step one-pot synthesis which is a reliable method of synthesizing the presented compounds. The starting reagents all possess sufficient solubility in acetone for the reaction to proceed though at a slower rate as generally syntheses were carried overnight. We found that refluxing often results in products containing impurities which can however be removed by flash chromatography. Room temperature reactions are thus preferred. The syntheses with chloro and bromo substituted ligands had excellent conversion rates and good yields but, reactions with 5,7-diiodo-8-hydroxyquinoline ligand were proven to be more tedious. While we were unable to replicate the synthesis of the organoruthenium-chlorido complex bearing this ligand (published by Hartinger *et al.*[32]) the reaction with the iodido ruthenium dimer resulted in moderately pure products only by using sodium acetate as base. Reactions with sodium methoxide generally resulted in the formation of at least three hydroxyquinoline species as determined by NMR.

The crystal structures reveal the expected typical piano-stool geometry (**Figure 2**) with the cymene ligand π -bonded to the central ruthenium ion while the remaining three coordination sites are occupied by the halido ligand and the N,O-bound hydroxyquinoline ligand in its deprotonated state. All bonds and angles are within the expected range of values for previously reported structures of compounds **3**[32] and **5**[32] as well as the previously reported structures of the organoruthenium complexes the parent (unsubstituted) ligand 8-hydroxyquinoline (8-hqH; **Table 3**).[32, 39, 40] Detailed crystallographic data is given in Table S1.

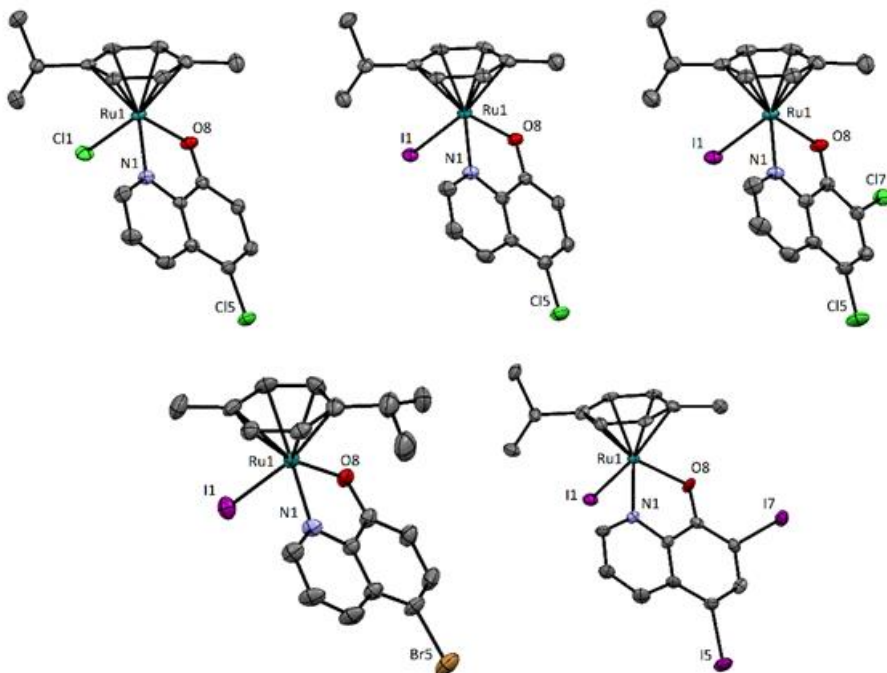


Figure 2: Crystal structures of compounds **1**, **6**, **7**, **9**, and **11** with heteroatom labelling. Thermal ellipsoids are shown at 40 % probability level. Hydrogen atoms and solvent molecules are omitted for better clarity of presentation.

Table 3: Bond lengths and N-Ru-O angle in ruthenium 8-hydroxyquinoline complexes with general formula $[\eta^6\text{-cymene}]\text{Ru}(\text{hq})\text{X}$; X = Cl, I.

	Ru-O	Ru-N	Ru-Cl	O-Ru-N
Ru-Cq ; [26]	2.075(3)	2.106(3)	2.427(1)	78.22(12)
$[\eta^6\text{-cymene}]\text{Ru}(8\text{-hq})\text{Cl}$; [40]	2.073(2)	2.094(2)	2.4219(7)	78.80
$[\eta^6\text{-cymene}]\text{Ru}(8\text{-hq})\text{Cl}$; [39]	2.076(2)	2.086(2)	2.4176(7)	78.90
$[\eta^6\text{-cymene}]\text{Ru}(8\text{-hq})\text{Cl}$; [32]	2.077(2)	2.096(2)	2.4245(6)	78.87
1	2.078(2)	2.093(2)	2.4147(5)	78.82(7)
3 ; [32]	2.063(1)	2.145(2)	2.4130(5)	78.55
5 ; [32]	2.11(1)	2.08(1)	2.429(3)	78.60
	Ru-O	Ru-N	Ru-I	O-Ru-N
6	2.073(2)	2.087(2)	2.7169(3)	78.95(8)
7	2.075(2)	2.088(3)	2.7262(4)	78.89(10)
9	2.080(3)	2.069(3)	2.7260(5)	78.47(12)
11	2.059(7)	2.091(9)	2.7327(11)	78.9(3)

3.2 Luminescence properties of selected ruthenium-hq complexes

It was previously reported that ruthenium-hydroxyquinolinato complexes exert fluorescence properties.[33] We have recorded fluorescence spectra in various solvents

(Table 2) and determined quantum yields for selected compounds. Both complexes **5** and **11** display analogous emission behaviors as previously reported. However, the ruthenium-hq complexes show inefficient fluorescence and only the quantum yield of complex **5** in CH₂Cl₂ is detectable (higher than 0.01 %). Ruthenium(II) tris-bipyridine (bpy) complex and related compounds have been proved to be efficient photosensitizers of singlet oxygen and thus utilized as anticancer reagents and we have therefore decided to check if our compounds also bear such potential. However, in this case it was established, that two selected compounds display negligible singlet oxygen production compared to [Ru(bpy)₃]²⁺. [41-43] The low luminescence efficiency and negligible SOG of the two complexes (Figure S1) might be ascribed to the non-irradiative decay of excited states or the poor excitation efficiency of these organometallic ruthenium complexes, which are different from analogues of complex [Ru(bpy)₃]²⁺. [44] Without SOG ability and photodynamic therapeutic activity, all these complexes were further investigated for their antitumor and antibacterial activity in normal condition without the photo-irradiation.

3.3 Effect of Ru complexes on cell viability in MG-63 and A549 cells.

To test the antitumor effect of Ru compounds, human MG-63 osteosarcoma cells and human A549 lung adenocarcinoma cells were exposed to the complexes **1, 2, 3, 4, 5, 8, 9, 10, 11, 12** during 24 h. The alteration in the energetic metabolism of the cells was determined by the MTT assay.

As can be seen in **Figure 3**, the complexes **1, 2, 4, 5, 8, 9, 10, 11, 12** caused an inhibitory effect on both cell lines in the range of 10 to 100 μM whereas the complex **3** only shows antiproliferative effects at higher concentration (100 μM).

Table 4: IC₅₀ values of ruthenium complexes against MG-63 and A549 cells after 24 h of incubation.

IC ₅₀ (μM)	MG-63 cells	A549 cells
1	24 ± 4	68 ± 5
2	15 ± 3	62 ± 3
3	>100 ±	>100 ±
4	17 ± 2	21 ± 2
5	8 ± 2	10 ± 1
8	50 ± 5	45 ± 4
9	24 ± 4	38 ± 5
10	8 ± 1	19 ± 3
11	49 ± 6	54 ± 6
12	9 ± 2	19 ± 3

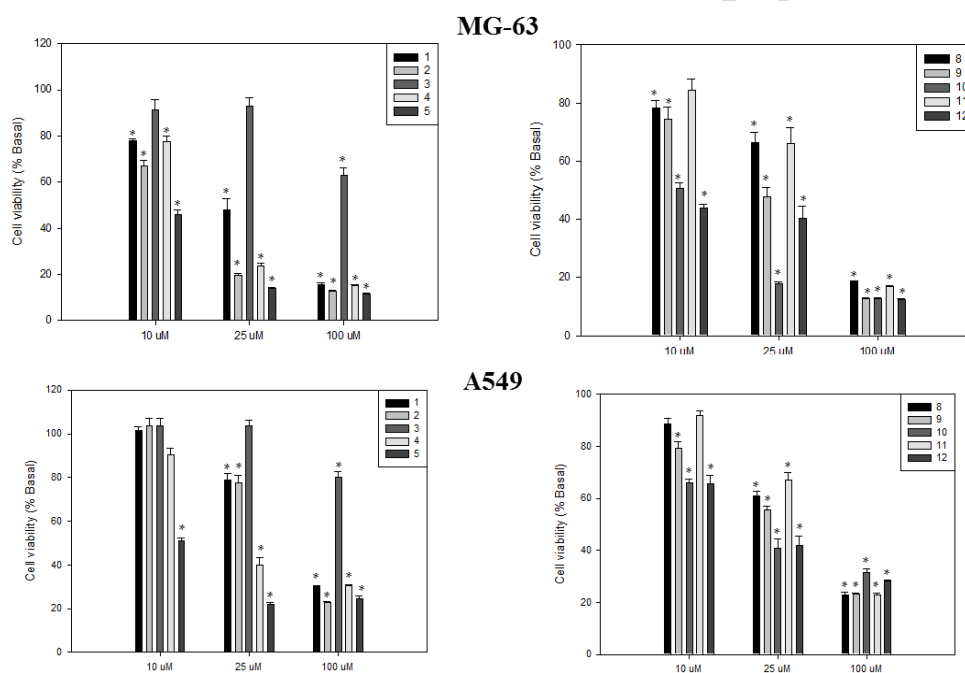


Figure 3: Effects of ruthenium complexes (**1–5**, **8–12**) on MG-63 human osteosarcoma cell line and A549 human lung adenocarcinoma proliferation. Cells were incubated in serum-free Dulbecco's modified Eagle's medium (DMEM) alone (control) or with different concentrations of ruthenium complexes (**1–5**, **8–12**) at 37 °C for 24 h. The results are expressed as the percentage of the basal level and represent the mean ± the standard error of the mean (SEM) (n = 18). *significant difference in comparison with the basal level (p<0.01)

Table 4 shows the IC₅₀ values for ruthenium compounds towards MG-63 and A549 cancer cells. As it can be seen ruthenium complexes produced their antitumor effects with the following increase of potency: **3** << **8**, **11** < **1**, **2** < **9** < **4**, **12** < **5**, **10**.

The results of the present study (**Figure 3** and **Figure 4**) confirm the findings of the Hartinger group on the relatively small influence of the halido ligand on the toxicity of the organoruthenium-hydroxyquinoline complexes. However, in contrast to that study our cytotoxicity assays (though on different cell lines) have shown that the halogen substitution pattern on the hq ligand itself does result in major changes in anticancer activity. The comparison of the anticancer activities suggests that the bromo substituents in position 5 and 7 of the quinoline ring play an important role in the antitumor activity of the ruthenium compounds (see complexes **5** and **10**). On the other hand, the presence of the methyl group in position 2 diminished the anticancer activity which proposes that this kind of ligands are detrimental for the anticancer activity of ruthenium compounds (see complexes **3** and **8**). The introduction of iodine instead of chlorine at position 2 improved slightly the anticancer activity against osteosarcoma and lung carcinoma cell lines (comparison between complex **3** and **8**). Our recent study on platinum(II)-hydroxyquinolinato complexes shows a very similar influence of the halogen-substitution pattern on the anticancer activity as in this case where the introduction of the bromo substituents on positions 5 and 7 resulted in increased toxicity in three different cell lines while the presence of the methyl substituent on position 2 resulted in a marked decrease.[45]

To determine the selectivity of antitumoral actions of complexes **9** and **10**, we performed new experiments using normal fibroblast cell line (MRC-5) and we compared its effects by calculating the selectivity index (SI). **Table 5** shows the higher selectivity of compound **10** than compound **9** on MG-63 cells. The SI values are 1.9 and 1.3 (MG-63 cells) for compounds **9** and **10**, respectively. Nevertheless, both compounds did not show selectivity actions on A549 cells (SI= 0.8).

Table 5: IC₅₀ and SI values of complexes **9** and **10** against MG-63 and A549 cells after 24 h of incubation.

IC ₅₀ (μM)	MG-63 cells	A549 cells	MRC-5 cells	SI _{MG-63}	SI _{A549}
9	24 ± 4	38 ± 5	31 ± 2	1.3	0.8
10	8 ± 1	19 ± 3	15 ± 2	1.9	0.8

Taking into consideration the higher antiproliferative action and cytotoxicity of complexes **9** and **10**, than that observed for other ruthenium compounds, we have decided to evaluate the antitumor actions of these complexes at lower times of incubation (3 and 6 h).

3.4 Effect of complexes 9 and 10 on cell viability in MG-63 and A549 cells.

To obtain deeper insight into the antiproliferative effects of complexes **9** and **10**, the cytotoxicity of these complexes at lower times was investigated through the reduction of MTT assay. In the **Figure 4** the effects of complexes **9** and **10** on the cell viability of MG-63 (A, B) and A549 cells (C, D) is shown. After 3 h, complex **10** impaired cell viability on MG-63 cells at 25 and 100 μM whilst the complex **9** only caused inhibitory effects at 100 μM. After 6 h of incubation, compound **10** provoked higher cytotoxicity than compound **9** (40 % survival vs 21 % survival). Besides, after 3 and 6 h both compounds increased the cytotoxicity levels in the range of 25-100 μM on A549 cells.

To explore the mode of cell death induced by complexes **9** and **10**, in the next step, we investigated the activation of apoptosis.

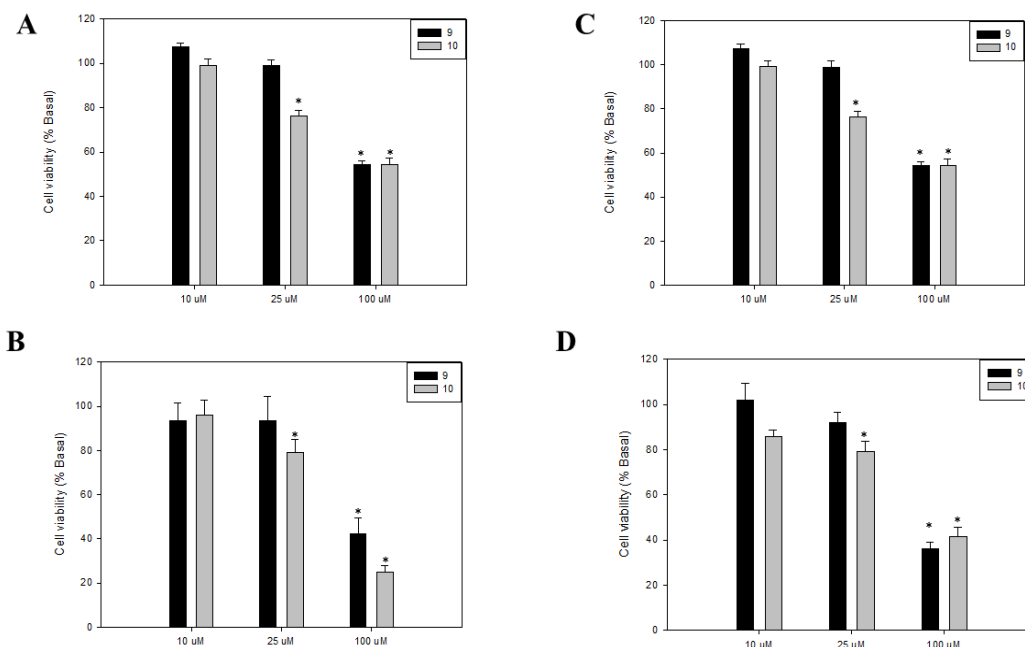


Figure 4: Effects of ruthenium complexes (**9** and **10**) on MG-63 human osteosarcoma cell line (A and B) and A549 human lung adenocarcinoma proliferation (C and D). Cells were incubated in serum-free Dulbecco's modified Eagle's medium (DMEM) alone (control) or with different concentrations of ruthenium complexes (**9** and **10**) at 37 °C for 3 (A, C) and 6 h (B, D). The results are expressed as the percentage of the basal level and represent the mean \pm the standard error of the mean (SEM) (n = 18). *significant difference in comparison with the basal level (p < 0.01)

3.5 Effect of complexes 9 and 10 on apoptosis induction in MG-63 and A549 cells.

Apoptosis is a physiological process of cell death enhanced in the presence of injurious agents. It produces several changes in the cell structure. As a consequence, a genetic program that leads to cell death is activated. Apoptosis is characterized by some morphological changes in the nucleus and the cytoplasm.[46] One of the first alterations that can be defined is the externalization of phosphatidylserine at the outer plasma membrane leaflet. Independently of the cell type and the nature of the harmful agent, the externalization of phosphatidylserine is always present in the earlier apoptotic events. Annexin V-FITC is a fluorescent probe with high affinity for phosphatidylserine, allowing its determination by fluorescence assays.

Figure 5 and **Figure 6** depict the flow cytometry results of the apoptotic process in the presence of complexes **9** and **10** (10, 25 and 100 μM) after 3 and 6 h of incubation in MG-63 and A549 cells respectively.

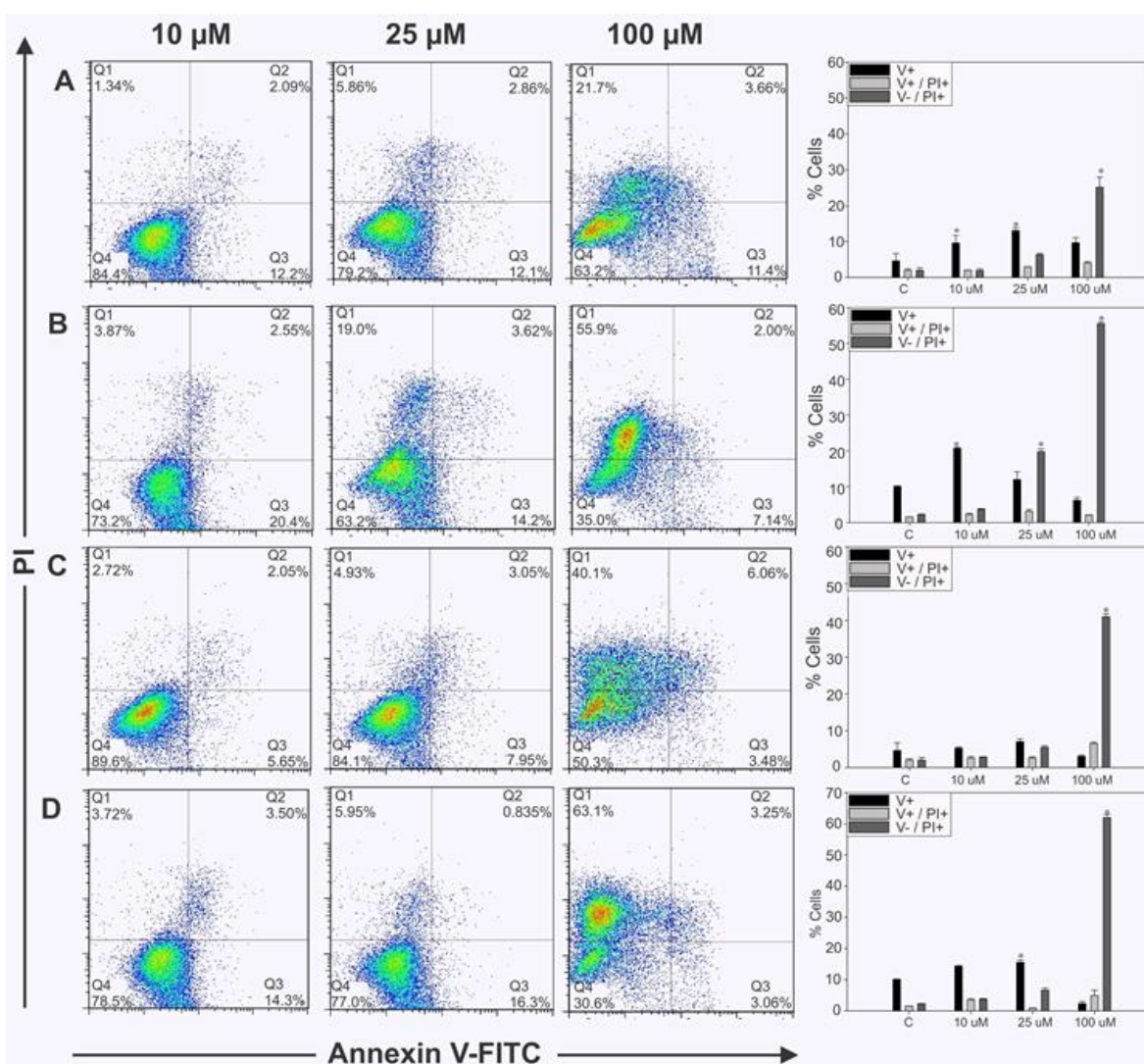


Figure 5: Effect of complexes **9** and **10** on the programmed cell death using flow cytometry in MG-63 cells. The cells were incubated with 10, 25 and 100 μM of the complex **9** during 3 (A) and 6 (B) h and complex **10** after 3 (C) and 6 (D) h. Plots are representative of three independent experiments. For each analysis 10,000 counts, gated on a FSC vs SSC dot plot, were recorded. Graphical bars show the percentage of Annexin V(+), V(+)/PI(+) and V(-)/PI(+) cells. Results are expressed as the mean ± SEM, n = 9, *significant differences vs. control (p < 0.01).

Figure 5A and **Figure 5C** show that after 3h of incubation of MG-63 cells, the control cultures showed 3 % of necrotic cells were annexin V negative / PI positive whilst the treatment with complexes **9** and **10** showed 24 % and 42% of necrotic cells at 100 μM, respectively. These results changed at 6 h (**Figure 5B** and **Figure 5D**), showing a substantial increase in the necrotic cellular fraction. After 6 h of treatment, complex **9** resulted in approximately 54 % of necrotic cells and complex **10** caused about 64 % of

necrotic cells suggesting that complex **10** has stronger antitumor effects than complex **9** on human osteosarcoma cells. As it can be seen, the percentages of apoptotic and apoptotic/necrotic cells increased with the concentration of both complexes and the exposure time. These results are in accordance with the viability assays (see **Figure 4**), confirming that the deleterious action of both complexes is dependent on their concentration.

On the other hand, **Figure 6A** and **Figure 6C** show that after 3 h of incubation of A549 cells, the basal condition showed 2 % of early apoptotic cells annexin V(+)/PI(-) and 1 % of late apoptotic cells annexin V(+)/PI(+) while after 3 h of incubation, complex **9** increased the levels of early apoptotic cells and late apoptotic cells (12 and 4 %, respectively) and the complex **10** showed 8 % of annexin V(+)/PI(-) and 5 % of annexin V(+)/PI(+), respectively.

After 6 h of treatment (**Figure 6B** and **Figure 6D**), complex **9** resulted in 76 % of early apoptotic cells and produced a striking increase in this fraction of apoptotic cells (16 %) whilst the compound **10** increased the level of early apoptotic cells annexin V(+)/PI(-) and late apoptotic cells annexin V(+)/PI(+) (20 % and 40 %, respectively) on A549 cells. These results are in agreement with the cell viability assays (**Figure 4**) suggesting the higher anticancer activity of complex **10** in comparison to complex **9**.

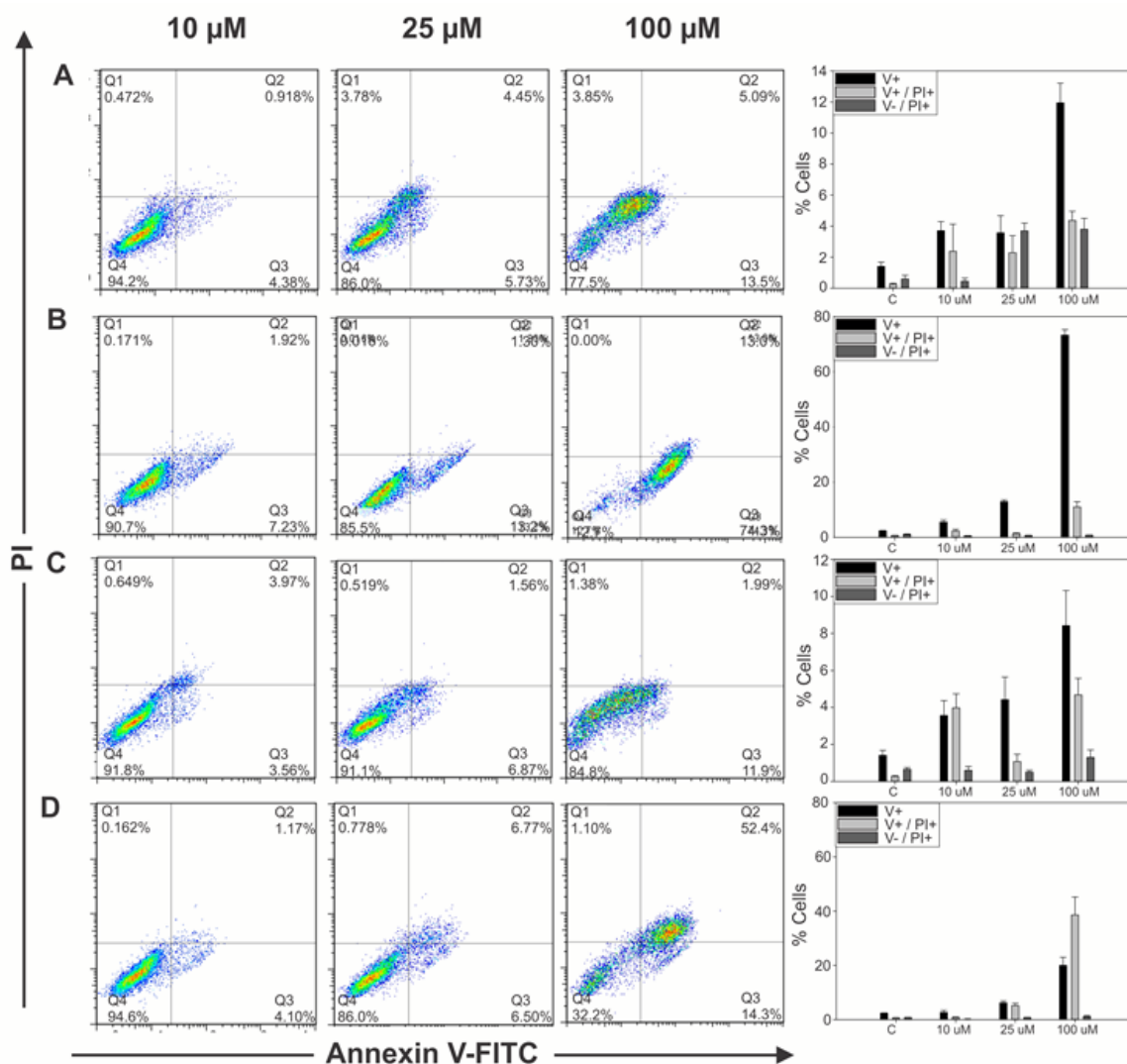


Figure 6: Effect of complexes **9** and **10** on the programmed cell death using flow cytometry in A549 cells. The cells were incubated with 10, 25 and 100 μM of the complex **9** during 3 (A) and 6 (B) h and complex **10** after 3 (C) and 6 (D) h. Plots are representative of three independent experiments. For each analysis 10,000 counts, gated on a FSC vs SSC dot plot, were recorded. Graphical bars show the percentage of Annexin V(+), V(+)/PI(+) and V(-)/PI(+) cells. Results are expressed as the mean \pm SEM, $n = 9$, *significant differences vs. control ($p < 0.01$).

3.6 Antibacterial activity

Due to the increasing problem of bacterial resistance to conventional agents, novel approaches will be soon necessary. Inclusion of metal fragments in the structures of established antibacterial agents can result in synergistic activity either by affecting different molecular targets or simply by acting as delivery systems.[47-49] In the case of our previous work with ruthenium complexes of quinolone antibacterial agents a loss of

antibacterial activity upon coordination to the organoruthenium fragment was observed.[20] Thus, we were interested to study if hydroxyquinolines retain their antibacterial activity when bound to ruthenium. Additional reason to study antibacterial potential of selected compounds is that chemotherapy commonly weakens the immune system. It would be desirable that in one compound both activities (anticancer and antibacterial) are present.[50] The in vitro antibacterial activity of the complexes **9** and **10** was carried out using *Escherichia coli*, *Bacillus cereus* and *Staphylococcus aureus* bacterial strains by micro-broth dilution method.

The results of the antibacterial screening are summarized in Table 6. Both compounds tested were found to have moderate antibacterial activity, complex **9** displayed strong inhibition action at MIC = 6.25 $\mu\text{g/mL}$ against strains *B. cereus* and *E. coli* whilst complex **10** exhibited stronger inhibition effects on *B. cereus* than *E. coli* (MIC = 6.8 $\mu\text{g/mL}$ and MIC = 10.2 $\mu\text{g/mL}$, respectively). Besides, compound **9** showed a slightly stronger antibacterial action than compound **10** toward *S. aureus* (MIC₉ = 14.6 $\mu\text{g/mL}$ vs MIC₁₀ = 15.4 $\mu\text{g/mL}$). In addition, to determine the effectiveness of compounds **9** and **10** as antibacterial agents we calculated the selectivity index (SI) considering the IC₅₀ values of complex **9** (19 $\mu\text{g/mL}$) and **10** (10.2 $\mu\text{g/mL}$) on normal fibroblast (MRC-5). The SI values showed that compound **9** exhibited in vitro antibacterial activities at non-cytotoxic concentrations against bacterial strains used in this study.

In this sense, it seems that the hydrogen atom at C7 plays an important role in the antibacterial activities. It is also worth to compare these results with antibacterial activity that was determined for some of our previously prepared ruthenium complexes. In our test with various Ru(III) compounds, weak activity (250 $\mu\text{g/mL}$) was only found for *mer*-[RuCl₃(dmsO-S)(phenanthroline)] whereas other tested compounds were not active.[51] In another study, antibacterial activity of organoruthenium(II) complex with antibacterial quinolone nalidixic acid was determined to be 23.8 $\mu\text{g/mL}$ which is higher from activities determined in this paper for complexes **9** and **10**. [20] It is clear that many factors govern the antibacterial properties of ruthenium complexes (e.g. oxidation state of metal; type of ligand, etc) and more data are needed to get a clearer picture.

Table 6: The *in vitro* antibacterial activity as MIC ($\mu\text{g/mL}$) and SI for compounds **9** and **10**.

Compounds	<i>E. coli</i>	<i>B. cereus</i>	<i>S. aureus</i>	SI <i>E.coli</i>	SI <i>B.cereus</i>	SI <i>S. aureus</i>
9	6.25	6.25	14.6	3.04	3.04	1.3
10	10.2	6.8	15.4	1	1.5	0.67

Furthermore, we would like also to mention that both compounds did not exert effects in preliminary tests on two fungi strains (*Candida albicans* and *Aspergillus niger*) in the tested concentration range (2.5 to 100 μM).

4. Conclusions

Novel ruthenium compounds as potential therapeutics currently require more intensive research to be more successful. Herein we thus present the continuation of our studies on organoruthenium-hydroxyquinolinato complexes with the optimization of synthetic procedures resulting in reliable and high-yield synthetic pathways, novel structural data for five different organoruthenium complexes and extensive biological evaluation of this series of compounds. The anticancer and antibacterial effects were investigated in order to evaluate the effects of the halogen substitution on positions 5 and 7 of the quinoline ring. Compounds were tested using human lung and bone cancer cells and *E. coli*, *B. cereus* and *S. aureus* bacterial strains.

In this order, the antibacterial effect of compound **9** was higher than compound **10** for all strains. Moreover, compounds **9** and **10** bearing bromo-substituted ligands impaired cell viability in a concentration-dependent manner showing stronger antiproliferative actions in human osteosarcoma than in lung adenocarcinoma cells. Nevertheless, the antiproliferative action of the complex **10** was more pronounced than compound **9** in bone and lung cancer cell lines. Therefore, combining previous knowledge with the *in vitro* anticancer activity screening, mode-of-action assays and determination of the toxicologic profile has resulted in the determination of lead compound **10** to be selected as candidate for undergoing preclinical *in vivo* experiments.

Acknowledgments

This work was supported by the Slovenian Research Agency (P-0175, Z1-6735, and bilateral Slovenian-Chinese project) and by UNLP (11X/690), CONICET (PIP 0034), and ANPCyT (PICT 2014-2223). We thank the EN-FIST Centre of Excellence, Ljubljana, Slovenia, for use of the SuperNova diffractometer.

Appendix A. Supplementary data

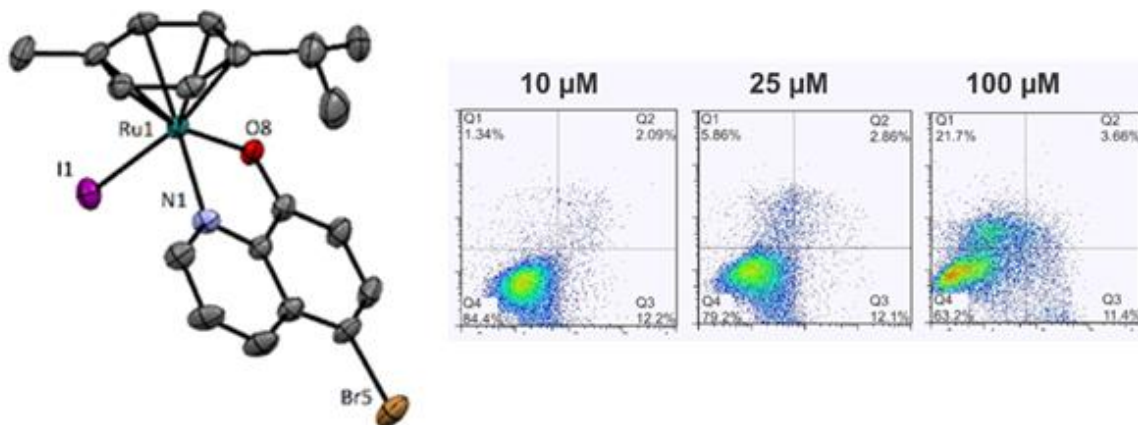
Supplementary data associated with this article can be found in the online version, at These data include: spectroscopic and analytical data of previously reported complexes **1**, **2**, **3**, **5**, **7**, **10**, **11**, **12**, crystallographic data table for compounds **1**, **6**, **7**, **9**, **11**, and luminescence measurements for compounds **5** and **11**.

References

- [1] J. Kljun, I. Turel, *Eur. J. Inorg. Chem.*, 2017, pp. 1655-1666.
- [2] S.H. Liang, A.G. Southon, B.H. Fraser, B.H. Krause-Heuer, B. Zhang, T.M. Shoup, R. Lewis, I. Volitakis, Y. Han, I. Greguric, A.I. Bush, N. Vasdev, *ACS Med. Chem. Lett.*, vol. 6, 2015, pp. 1025-1029.
- [3] D.A. Williams, T.L. Lemke (Eds.), *Foye's principles of medicinal chemistry*, Lippincott Williams & Wilkins, 2002.
- [4] V. Prachayasittikul, S. Prachayasittikul, S. Ruchirawat, V. Prachayasittikul, *Drug Des. Devel. Ther.*, vol. 7, 2013, pp. 1157-1178.
- [5] S. Tardito, A. Barilli, I. Bassanetti, M. Tegoni, O. Bussolati, R. Franchi-Gazzola, C. Mucchino, L. Marchio, *J. Med. Chem.*, vol. 55, 2012, pp. 10448-10459.
- [6] J.A. Jacobsen, J.L. Fullagar, M.T. Miller, S.M. Cohen, *J. Med. Chem.*, vol. 54, 2011, pp. 591-602.
- [7] K.E.S. Matlack, D.F. Tardiff, P. Narayan, S. Hamamichi, K.A. Caldwell, G.A. Caldwell, S. Lindquist, *Proc. Nat. Acad. Sci. U. S. A.*, vol. 111, 2014, pp. 4013-4018.
- [8] C. Supan, G. Mombo-Ngoma, M.P. Dal-Bianco, C.L.O. Salazar, S. Issifou, F. Mazuir, A. Filali-Ansary, C. Biot, D. Ter-Minassian, M. Ramharter, P.G. Kremsner, B. Lell, *Antimicrob. Agents Chemother.*, vol. 56, 2012, pp. 3165-3173.
- [9] C. Biot, F. Nosten, L. Fraise, D. Ter-Minassian, J. Khalife, D. Dive, *Parasite*, vol. 18, 2011, pp. 207-214.
- [10] F. Dubar, J. Khalife, J. Brocard, D. Dive, C. Biot, *Molecules*, vol. 13, 2008, pp. 2900-2907.
- [11] M. Patra, G. Gasser, *Nat. Rev. Chem.*, vol. 1, 2017, pp. art. no. 0066.
- [12] O. Domotor, S. Aicher, M. Schmidlehner, M.S. Novak, A. Roller, M.A. Jakupec, W. Kandlioller, C.G. Hartinger, B.K. Keppler, E.A. Enyedy, *J. Inorg. Biochem.*, vol. 134, 2014, pp. 57-65.

- [13] M. Carcelli, A. Bacchi, P. Pelagatti, G. Rispoli, D. Rogolino, T.W. Sanchez, M. Sechi, N. Neamati, *J. Inorg. Biochem.*, vol. 118, 2013, pp. 74-82.
- [14] Y. Lin, Y. Huang, W. Zheng, F. Wang, A. Habtemariam, W. Luo, X. Li, K. Wu, P.J. Sadler, S. Xiong, *J. Inorg. Biochem.*, vol. 128, 2013, pp. 77-84.
- [15] M. Schmidlehner, L.S. Flocke, A. Roller, M. Hejl, M.A. Jakupec, W. Kandioller, B.K. Keppler, *Dalton Trans.*, vol. 45, 2016, pp. 724-733.
- [16] W. Kandioller, A. Kurzwernhart, M. Hanif, S.M. Meier, H. Henke, B.K. Keppler, C.G. Hartinger, *J. Organomet. Chem.*, vol. 696, 2011, pp. 999-1010.
- [17] S.B. Murray, V.M. Babak, G.C. Hartinger, J.P. Dyson, *Coord. Chem. Rev.*, vol. 306, 2016, pp. 86-114.
- [18] I. Turel, M. Pecanac, A. Golobic, E. Alessio, B. Serli, A. Bergamo, G. Sava, *J. Inorg. Biochem.*, vol. 98, 2004, pp. 393-401.
- [19] I. Turel, B. Andersen, E. Sletten, A.J.P. White, D.J. Williams, *Polyhedron*, vol. 17, 1998, pp. 4195-4201.
- [20] R. Hudej, J. Kljun, W. Kandioller, U. Repnik, B. Turk, C.G. Hartinger, B.K. Keppler, D. Miklavcic, I. Turel, *Organometallics*, vol. 31, 2012, pp. 5867-5874.
- [21] J. Kljun, A.K. Bytcek, W. Kandioller, C. Bartel, M.A. Jakupec, C.G. Hartinger, B.K. Keppler, I. Turel, *Organometallics*, vol. 30, 2011, pp. 2506-2512.
- [22] I. Turel, J. Kljun, F. Perdih, E. Morozova, V. Bakulev, N. Kasyanenko, J.A.W. Byl, N. Osheroff, *Inorg. Chem.*, vol. 49, 2010, pp. 10750-10752.
- [23] J. Kljun, A.J. Scott, T. Lanišnik Rižner, J. Keiser, I. Turel, *Organometallics*, vol. 33, 2014, pp. 1594-1601.
- [24] J. Kljun, M. Anko, K. Traven, M. Sinreih, Ž. Ude, E.E. Codina, J. Stojan, T. Lanišnik Rižner, I. Turel, *Dalton Trans.*, vol. 45, 2016, pp. 11791-11800.
- [25] A. Mitrović, J. Kljun, I. Sosič, S. Gobec, I. Turel, J. Kos, *Dalton Trans.*, vol. 45, 2016, pp. 16913-16921.
- [26] M. Gobec, J. Kljun, I. Sosič, I. Mlinarič-Raščan, M. Uršič, S. Gobec, I. Turel, *Dalton Trans.*, vol. 43, 2014, pp. 9045-9051.
- [27] P.A. Adlard, R.A. Cherny, D.I. Finkelstein, E. Gautier, E. Robb, M. Cortes, I. Volitakis, X. Liu, J.P. Smith, K. Perez, K. Laughton, Q.X. Li, S.A. Charman, J.A. Nicolazzo, S. Wilkins, K. Deleva, T. Lynch, G. Kok, C.W. Ritchie, R.E. Tanzi, R. Cappai, C.L. Masters, K.J. Barnham, A.I. Bush, *Neuron*, vol. 59, 2008, pp. 43-55.
- [28] C. Martin Santos, S. Cabrere, C. Rios-Luci, J.M. Padron, I. Lopez Solera, A.G. Quiroga, M.A. Medrano, C. Navarro-Ranninger, J. Aleman, *Dalton Trans.*, vol. 42, 2013, pp. 13343-13348.
- [29] D.C. Reis, M.C.X. Pinto, E.M. Souza-Fagundes, L.F. Rocha, V.R.A. Pereira, C.M.L. Melo, H. Beraldo, *Biometals*, vol. 24, 2011, pp. 595-601.
- [30] W.Q. Ding, S.E. Lind, *Iubmb Life*, vol. 61, 2009, pp. 1013-1018.
- [31] B. Mirković, B. Markelc, M. Butinar, A. Mitrović, I. Sosič, S. Gobec, O. Vasiljeva, B. Turk, M. Čemežar, G. Serša, J. Kos, *Oncotarget*, vol. 6, 2015, pp. 19027-19042.
- [32] M. Kubanik, H. Holtkamp, T. Söhnle, S.M.F. Jamieson, C.G. Hartinger, *Organometallics*, vol. 34, 2015, pp. 5658-5668.
- [33] M. Malipeddi, C. Lakhani, M. Chhabra, P. Paira, R. Vidya, *Bioorg. Med. Chem. Lett.*, vol. 25, 2015, pp. 2892-2896.
- [34] T.T. Thai, B. Therrien, G. Suss-Fink, *J. Organomet. Chem.*, vol. 694, 2009, pp. 3973-3981.
- [35] A. Altomare, G. Cascarano, C. Giacovazzo, A.C. Guagliardi, M.C. Burla, G. Polidori, M. Camalli, *J. Appl. Cryst.*, vol. 27, 1994, pp. 435.
- [36] G.M. Sheldrick, *Acta Crystallogr., Sect. A*, vol. 64, 2008, pp. 112-122.
- [37] C.F. Macrae, P.R. Edgington, P. McCabe, E. Pidcock, G.P. Shields, R. Taylor, M. Towler, J. van De Streek, *J. Appl. Cryst.*, vol. 39, 2006, pp. 453-457.
- [38] T. Mosmann, *J. Immunol. Methods*, vol. 65, 1983, pp. 55-63.

- [39] A. Habtemariam, M. Melchart, R. Fernandez, S. Parsons, I.D.H. Oswald, A. Parkin, F.P.A. Fabbiani, J.E. Davidson, A. Dawson, R.E. Aird, D.I. Jodrell, P.J. Sadler, *J. Med. Chem.*, vol. 49, 2006, pp. 6858-6868.
- [40] C. Gemel, R. John, C. Slugove, K. Mereiter, R. Schmid, K. Kirchner, *J. Chem. Soc.-Dalton Trans.*, 2000, pp. 2607-2612.
- [41] C.-T. Poon, P.-S. Chan, C. Man, F.-L. Jiang, R.N.S. Wong, N.-K. Mak, D.W.J. Kwong, S.-W. Tsao, W.-K. Wong, *J. Inorg. Biochem.*, vol. 104, 2010, pp. 62-70.
- [42] H. Yin, M. Stephenson, J. Gibson, E. Sampson, G. Shi, T. Sainuddin, S. Monro, S.A. McFarland, *Inorg. Chem.*, vol. 53, 2014, pp. 4548-4559.
- [43] M.C. DeRosa, R.J. Crutchley, *Coord. Chem. Rev.*, vol. 233-234, 2002, pp. 351-371.
- [44] H. Huang, B. Yu, P. Zhang, J. Huang, Y. Chen, G. Gasser, L. Ji, H. Chao, *Angew. Chem. Int. Ed.*, vol. 54, 2015, pp. 14049-14052.
- [45] M.D. Živković, J. Kljun, T. Ilić-Tomić, A. Pavić, A. Veselinović, D.D. Manojlović, J. Nikodinović-Runić, I. Turel, *Inorg. Chem. Front.*, vol. 5, 2018, pp. 39-53.
- [46] S. Elmore, *Toxicol. Pathol.*, vol. 35, 2007, pp. 495-516.
- [47] J.A. Lemire, J.J. Harrison, R.J. Turner, *Nat. Rev. Microbiol.*, vol. 11, 2013, pp. 371-384.
- [48] E. Alessio (Ed.), *Bioinorganic Medicinal Chemistry*, Wiley-VCH Verlag & Co. KGaA, Weinheim, Germany, 2011.
- [49] J.R. Schwartz, *J. Drugs Dermatol.*, vol. 15, 2016, pp. 140-144.
- [50] K.E. de Visser, A. Eichten, L.M. Coussens, *Nat. Rev. Cancer*, vol. 6, 2006, pp. 24-37.
- [51] I. Turel, A. Golobič, J. Kljun, P. Samastur, U. Batista, K. Sepčić, *Acta Chim. Slov.*, vol. 62, 2015, pp. 337-345.



Herein we present the study of the cytotoxic potential and apoptosis induction of a series of organoruthenium 8-hydroxyquinolinato complexes. Bromo substituted ligands gave best preliminary cytotoxicity results. Apoptosis induction results are in agreement with the cell viability assays. The most toxic compounds displayed IC_{50} values in the low micromolar range.

Highlights:

- Synthesis, characterization and biological evaluation of twelve organoruthenium–8-hydroxyquinolinato (**Ru-hq**) complexes
- Investigation of anticancer and antibacterial activity
- Study of apoptosis induction
- Incorporation of bromo substituents on ligand is highly beneficial